Analytical Methods

Accepted Manuscript

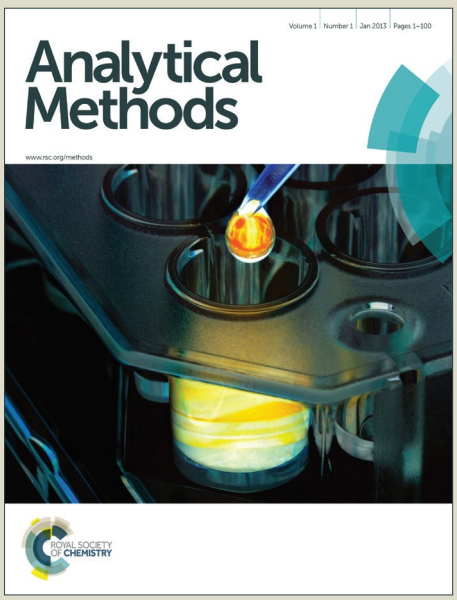

This is an *Accepted Manuscript*, which has been through the Royal Society of Chemistry peer review process and has been accepted for publication.

Accepted Manuscripts are published online shortly after acceptance, before technical editing, formatting and proof reading. Using this free service, authors can make their results available to the community, in citable form, before we publish the edited article. We will replace this *Accepted Manuscript* with the edited and formatted *Advance Article* as soon as it is available.

You can find more information about *Accepted Manuscripts* in the Information for Authors.

Please note that technical editing may introduce minor changes to the text and/or graphics, which may alter content. The journal's standard Terms & Conditions and the Ethical guidelines still apply. In no event shall the Royal Society of Chemistry be held responsible for any errors or omissions in this *Accepted Manuscript* or any consequences arising from the use of any information it contains.

ROYAL SOCIETY OF CHEMISTRY

www.rsc.org/methods

Journal Name

ARTICLE

A green synthesis of high fluorescence nitrogen-doped graphene quantum dots for the highly sensitive and selective detection of mercury (II) ions and biothiols

Received 00th January 20xx,
Accepted 00th January 20xx

DOI: 10.1039/x0xx00000x

www.rsc.org/

Zhengyu Yan, Xincheng Qu, Qianqian Niu, Chunqing Tian, Chuanjian Fan and Baofen Ye*

A facile and environment-friendly strategy to prepare nitrogen-doped graphene quantum dots (N-GQDs) with high quantum yield of 28.10% was reported. The obtained N-GQDs exhibited strong blue fluorescence emission with the maximum emission and excitation at 450 nm and 355 nm, respectively. Taking advantage of the effective quenching effect of Hg^{2+} to N-GQDs, such N-GQDs was developed for the efficient and sensitive detection of Hg^{2+} with a relatively low detection limit of 0.032 μM. Based on the selective coordination of biothiols and Hg^{2+}, the fluorescence of the N-GQDs/Hg system was recovered with the addition of biothiols. This fluorescence "Off-On" process showed a sensitive response to biothiols with a detection limit of 0.036 μM for cysteine and 0.034 μM for glutathione. Most importantly, the N-GQDs-based fluorescence method was successfully used to monitor Hg^{2+} in real water samples and biothols in serum samples.

Introduction

The accumulation of heavy-metal ions in the environment has generated considerable concern because of their strong toxicity, bioaccumulation, and a health risk even at a very low concentration[1]. Mercury (II) ions (Hg^{2+}), one of the most toxic heavy metals, are well-known bioaccumulative and nonbiodegradable pollutants in the ecosystem. The accumulation of Hg^{2+} in the organisms can cause severe health problems such as nervous damage, kidney failure, and liver disorder[2]. Therefore, routine detection of Hg^{2+} is of great necessity. Conventional analytical techniques for Hg^{2+} detection include atomic absorption[3], ICP-MS[4] and so on. Although these methods are very sensitive and selective, they usually require expensive instrument, complicated sample preparation or sophisticated operations which limited their application in rapid and user-friendly routine Hg^{2+} monitoring[5]. Thus, it is still highly desirable to develop a simple, sensitive, and selective method for Hg^{2+} detection.

On the other hand, low-molecular-weight biothiols, for example, cysteine (Cys) and glutathione (GSH) play crucial roles in the biological processes such as reversible redox reactions and cellular functions[6, 7]. Abnormal levels of biothiols in human serum and urine are linked with many disease including developmental retardation, encephaledema, skin lesions, and liver injuries, etc[8-10]. Therefore, increasing attention has been drawn to sensitive and selective detection of biothiols for human health. Conventional analytical methods, such as the electro-chemical[11], colorimetric[12], fluorometric[13], high-performance liquid chromatography(HPLC)[14], surface enhanced Raman scattering (SERS)[15] and mass spectrometry techniques[16], have been developed to determine Cys and GSH over the years. Much effort has been made to develop fluorescence sensors because of its simple operation, high sensitivity, and adaptability for in-field measurement[17]. A number of novel biothiol fluorescence sensor based on advanced materials have also been developed in recent years.

More recently， two kinds of emerging carbon nanomaterial, graphene oxide (GO)[18, 19], and graphene quantum dots (GQDs)[20-22],have drawn increasing attention in sensor application. especially GQDs, a type of graphene sheet with a size less than 100 nm[23], have attracted remarkable interest as a promising nanomaterial for fluorescence sensing of Hg^{2+} and biothiols[24]. Compared to traditional semiconductor quantum dots, GQDs are superior in terms of high biocompatibility ,low toxicity, chemical inertness, and aqueous solubility[25]. Various strategies such as mechanical carving from graphene[26], electrochemical synthesis[27] and chemical oxidation[28] have been developed for the synthesis of GQDs. In general, these processes need multi-step operations and post-treatments. Recently, Dong's group reported a simple and economic bottom–up method for the preparation of GQDs using citric acid with a quantum yield of 9.0%[29]. Shen et al proposed a facile graphene oxide reduction with PEG surface passivation method for the preparation of GQDs with a quantum yield of 7.4%[26]. However, low quantum yields of the as-synthesized GQDs is still remained to be solved. Heteroatom doping is a well-known route to tune the intrinsic properties of carbon nanomaterials. Nitrogen-doped graphene quantum dots (N-GQDs) was firstly reported by Qu et al in 2011[30] by a simple electrochemical approach. Since then, nitrogen atom doping have received significant attention because the quantum confinement and the edge effect of the nitrogen atom can

Key Laboratory of Biomedical Functional Materials, School of Science, China Pharmaceutical University. Tongjia Xiang 24, Nanjing, Jiangsu, 210009, P.R. China.E-mail:baofen_ye@163.com

† Electronic Supplementary Information (ESI) available: Fig. S1, S2 See DOI: 10.1039/x0xx00000x .

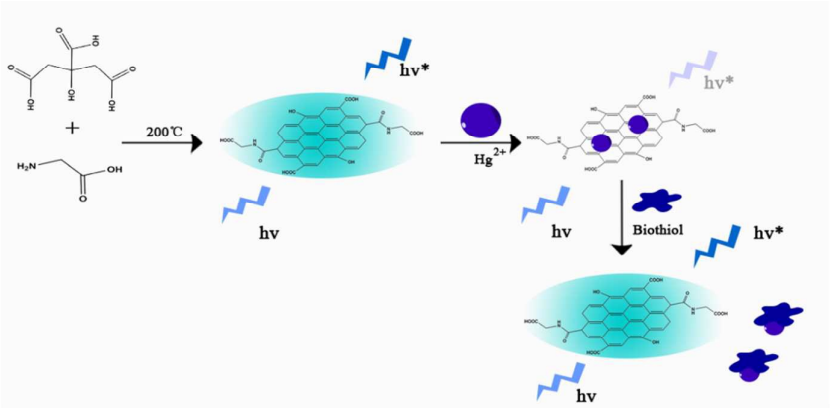

Scheme. 1 The schematic illustration of the mechanism of the N-GQD based detection process for Hg^{2+} and biothiols.

significantly enhance their fluorescence properties. Recently, several routes have been proposed to doping chemically bonded nitrogen atoms into GQDs frame work. Li et al applied the solution chemistry approach to synthesis of N-GQDs, which required strict anhydrous condition and sophisticated operations[31]. Cai et al used a relatively simple but time-consuming method to synthesis of N-GQDs[32]. Therefore, it is still necessary to further develop simple and low-cost methods for N-GQDs with high quantum yields and novel applications.

Herein, we report a relatively facile and environment-friendly one-pot method to prepare water-soluble N-GQDs by using citric acid (CA) and glycine (Gly) as carbon and nitrogen sources respectively. The as-prepared N-GQDs have a size around 1~4 nm and exhibit blue fluorescence with a high quantum yield of 28.1 %, which is far higher than the quantum yield of GQDs simply prepared by citric acid (CA). Meanwhile, owing to the coordination occurring between Hg^{2+} and functional groups on surface of N-GQDs, the fluorescence of N-GQDs was quenched efficiently (Scheme 1). This fluorescence "turn-off" process makes it possible to label-free sensitive and selective detect Hg^{2+} with a detection limit of 0.032 μM. With the addition of Cys and GSH, the fluorescence of the N-GQDs/Hg^{2+} system is recovered gradually because of their selective affinities with Hg^{2+} through Hg-S bonding interactions. Correspondingly, the fluorescence "turn-on" process takes place. The application of N-GQDs in the detection of Hg^{2+} and biothiols in real samples is also successfully demonstrated.

2 Experimental

2.1 Materials

Citric acid monohydrate(CA), glycine(Gly), cysteine, Larginine, alanine, serine, isoieucine, proline, leucine, glutamic acid, phenylalanine, valine, histidine, sliver nitrate, sodium dihydrogen phosphate and disodium hydrogen phosphate were obtained from Sinopharm Chemical Reagent Co., Ltd. (Shanghai, China). Glutathione reduced was obtained from Aladdin Chemistry Co., Ltd. (Shanghai, China). Mercury perchlorate trihydrate was obtained from Alfa Aesar China (Tianjin,China) Co., Ltd. Iron choloride hexahydrated, zinc chloride, cupric sulfate, calcium chloride anhydrous, magnesium sulfate anhydrous were obtained from Nanjing Chemical Reagent Co., Ltd(Nanjing,China). Barium chloride, lead nitrate, cadmium acetate, cobaltous chloride, nickelous sulfate, aluminum chloride were obtained from ShangHai LingFeng Industry Co., Ltd (Shanghai,China). Phosphate buffer solutions (PBS) of various pH were self-prepared. All other reagents were of analytical reagent grade and used as received.

2.2 Apparatus

Fluorescence spectra were recorded on a RF-5301 spectrofluorimeter (Shimatdzu China Co., Ltd., Beijing, China) with an excitation wavelength of 355 nm. Excitation and emission slit widths were 5 nm. Quartz cuvettes with 1-cm path length were used for fluorescence and UV-vis spectra measurements. UV–vis absorption spectra were recorded on a UV-2100 UV–vis spectrometer (Beijing Beifen-Ruili Analytical Instrument Group Co., Ltd., Beijing, China). pH measurements were achieved by a pHS-25 pH meter (Shanghai Leici Chuangyi Apparatus & Instrument Co., Ltd. Shanghai, China). Transmission electron micrograph (TEM) images were recorded by a JEOL-2010 electron microscope (JEOL Ltd, Tokyo, Japan) operating at an accelerating voltage of 200 kV. X-ray photoelectron spectroscopy (XPS) measurements were performed on PHI 5000 Versa Probe (ULVAC-PHI, Ltd, Japan).

2.3 Synthesis of the N- GQDs

N-GQDs were prepared by the pyrolysis of CA and Gly following a reported procedure[29]. The reported procedure used CA as carbon source individually and the quantun yield of the obtained GQDs was relatively low. In order to improve the quantum yield, nitrogen doping was applied and Gly was used as nitrogen source simultaneously. Briefly, CA (2.0 g) and Gly (0.5 g) were placed in a 25 ml round bottom flask. The flask was heated to 200 °C by using a heating mantle under stirring. The mixture was melted within 5 min and the color of the melt turned from colorless to yellow, orange and then dark brown for about 20 min. The dark brown product indicated the formation of N-GQDs. Then the obtained liquid was added 100 ml of 10 $mgmL^{-1}$ NaOH drop by drop with vigorous stirring and adjusted the pH of the N-GQDs solution to 7.5. The final obtained

Table. 1 QY of the N-GQDs

Gly (mg): CA (mg)	Fluorescence intensity (*I*)	Abs (*A*)	QY (%)
0:0	472.551	0.054	4.52
8:1	823.464	0.044	14.21
8:2	725.002	0.058	28.10
8:4	357.489	0.051	27.23
8:6	221.890	0.044	25.80
8:8	549.027	0.054	22.92

N-GQDs solution was stored in the dark at 4 °C for further characterization and use.

2.4 Fluorescence Quantum yield (QY) measurement

The QY of N-GQDs was measured according to an established procedure. Quinine sulphate (literature QY 0.54 [33]) was chosen as the standard sample for the determination of the QY of N-GQDs. The value of QY was calculated according to the following equation:

$$Y_u = Y_s \bullet \frac{F_u}{F_s} \bullet \frac{A_s}{A_u} \bullet \frac{n_u^2}{n_s^2} \qquad (1)$$

Where *Y* is the quantum yield, *F* is the measured integrated emission intensity, n is the refractive index of the solvent (1.33 for water), and *A* is the optical density. The subscript "*S*" refers to the reference standard with known QY and "*u*" for the sample.

2.5 Detection of Hg^{2+} by N- CQDs

The detection of Hg^{2+} was performed in PBS buffer solution (10mM, pH 7.5) at room temperature. In a typical process, different amounts of Hg^{2+} were added into the mixture of 3 μL N-GQDs (0.24 mg mL^{-1}) and 1800 μL PBS buffer (10 mM, pH 7.5). The solution was diluted with water to 2.0 mL with the final Hg^{2+} concentration of 0-10 μM and mixed thoroughly. After incubating at room temperature for 20 min, the fluorescence measurements were carried out.

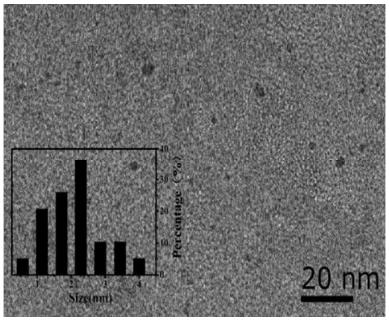

Figure. 1 TEM image of the obtained N-GQDs. Inset: Particle size distribution histogram.

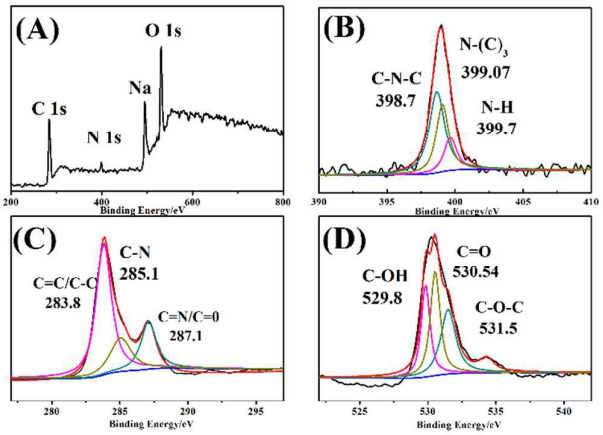

Figure.2 XPS (A), N 1s (B), C 1s (C) and O 1s spectra (D) of the obtained N-GQDs.

2.6 Real water sample preparation

To evaluate the N-GQDs-based sensor for Hg^{2+} detection in an artificial system, the performance of the present method for real water sample analysis was examined by three kinds of water samples. Pure water was obtained from Hangzhou Wahaha Group Co., Ltd, tap water sample was obtained from our lab and the lake water was collected from Ming Lake in China Pharmaceutical University campus. All the water samples were first centrifuged at 8000 rpm for 10 min, and then the clear supernatant layer was filtered through a 0.45 μm Millipore filter[21]. The resultant water samples were spiked Hg^{2+} at different concentration levels and then analyzed with the proposed method.

2.7 Detection of biothiols by the quenched N-GQDs

Different amounts of biothiols (Cys or GSH) were added into the N-GQDs/ Hg^{2+} solution (the Hg^{2+} concentration is 77.0 μM). After incubating at room temperature for 20 min, the fluorescence

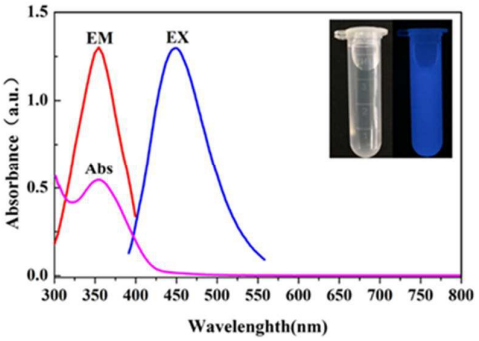

Figure. 3 UV-vis and fluorescence spectra of the N-GQDs. Inset: photographs taken under day light (left) and 365 nm UV light (right)

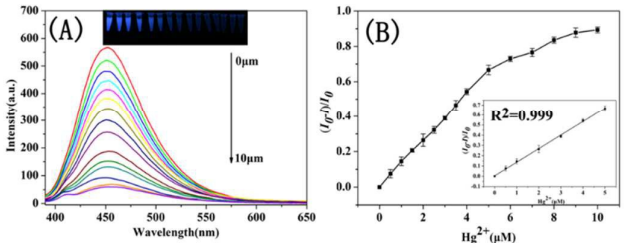

Figure. 4 (A) Fluorescence emission spectra of the N-GQDs in PBS (pH 7.5) upon addition of various concentrations of Hg^{2+} (from top to bottom: 0 μM, 0.5 μM, 1 μM, 1.5 μM, 2.0 μM, 2.5 μM , 3.0 μM, 3.5 μM, 4.0 μM, 5.0 μM, 6.0 μM, 7.0 μM, 8.0 μM, 9.0 μM and 10.0 μM), excitated at 355 nm. Inset: Photographs of the N-GQDs containing of various concentration of Hg^{2+} under UV light. (B) The linear relationship between $(I_0\text{-}I)/ I_0$ with the Hg^{2+} concentrations in the range from 0 to 5.0 μM. I_0 and I are the emission fluorescence intensities of N-GQDs at 450 nm in the absence and presence of Hg^{2+}, respectively.

measurement were carried out.

2.8 Human serum sample preparation

Fresh human serum samples were supplied from three healthy adult volunteers at a local hospital and stored frozen until assay. In order to eliminate the interferences of proteins, acetonitrile were added in serum samples (CH3CN: serum=1:1). After vortexing for 2 min, the mixture was centrifuged at 10000 rpm for 10 min. Then the supernatant layer was filtered through a 0.45 μm Millipore filter for further analysis[24]. The assay solution were spiked with known concentration of Cys following the standard addition method. The total quantities of Cys recovery, the recovery rate and the standard deviation values were obtained. All the experiments were performed in compliance with the relevant laws and institutional guidelines, and approved by the relevant institutional committees (Ethics Committee of China Pharmaceutical University). Informed consent was obtained

Table. 2 Determination results of Hg^{2+} in real water samples

Samples	Added (μM)	Found (μM)	RSD (%, n=3)	Recovery (%)
Pure water	1.00	0.93	0.7	93.0
	2.00	1.79	2.8	89.5
	3.00	3.00	1.3	100.0
Tap water	1.00	0.96	3.5	96.0
	2.00	1.95	2.7	97.5
	3.00	2.59	7.7	86.3
Water of Ming lake	1.00	0.83	2.3	83.0
	2.00	2.17	5.9	100.8
	3.00	2.92	0.5	97.3

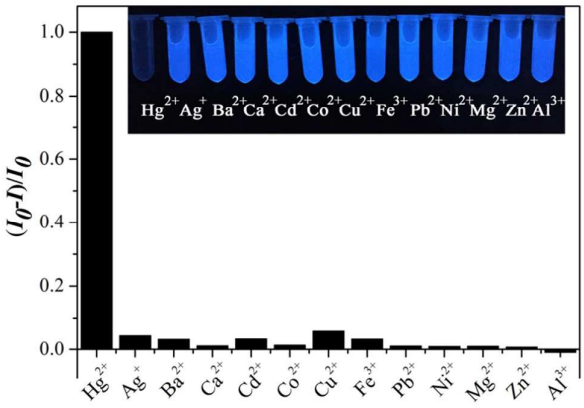

Figure. 5 Relative fluorescence intensity at maximum excitation wavelength 355 nm of N-GQDs solution in the presence of 10.0 μM of various metal ions. Inset: Photographs of the N-GQDs containing 100.0 μM of various metal ions under UV light.

for all experiments involving human subjects.

3 Results and Discussions

3.1 Characterization of N-GQDs

In the present study, the water dispersible N-GQDs were prepared by a one-pot pyrolysis of CA as carbon source and Gly as nitrogen source at 200 °C. The morphology of the N-GQDs was characterized with TEM. As shown in Figure. 1, the obtained N-GQDs are fairly uniform and well dispersed. 22 N-GQD particles were randomly selected to measure the particle size and the particle size distribution histogram was shown in Figure. 1 inset. The as-prepared N-GQDs exhibit an average size of 2.2± 1.5 nm, which is closed to that of the reported GQDs in literature[34].The composition of the N-GQDs was then investigated by XPS measurement. The full range XPS analysis of the N-GQDs sample clearly showed the presence of C 1s, N 1s and O 1s (Figure. 2A). The C 1s, N 1s and O 1s peaks centered at 283.9 ev 399 ev and 530.3 ev, respectively. This confirmed the successful nitrogen doping of GQDs[35]. The peak at 495.0 ev was attributed to Na 1s which is from NaOH. The high resolution C 1s XPS spectra of N-GQDs (Figure. 2C) indicated that there were three peaks at 283.8 ev, 287.1 ev and 288.1 ev, which were corresponding to C=C/C-C bonding in graphene, C=N/C=O and C-N groups, respectively[22]. The high resolution N 1s spectra of the N-GQDs (Figure. 2B) exhibited three peaks at 398.7 ev, 399.1 ev and 399.7 ev, which were attributed to the pyrrole like C-N-C, and graphitic N-$(C)_3$ and N-H groups, suggesting that nitrogen atoms were incorporated into the carbon-carbon bonds of the graphene[34]. The high resolution O 1s spectra of the N-GQDs (Figure . 2D) was deconvoluted into three peaks, which were assigned to C-OH at 529.8 ev, C=O at 530.5 ev and C-O-C at 531.5 ev and indicated that the N-GQDs were rich in hydroxyl, carbonyl and carboxylic acid groups on the surface and edges[36]. The composition of the obtained N-GQDs was also evaluated by the elemental analysis. The results

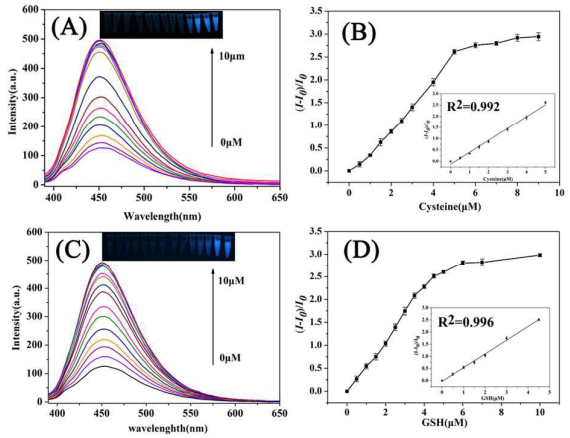

Figure. 6 Fluorescence emission spectra of the N-GQDs/ Hg^{2+} in PBS buffer (pH 8.0) upon addition of various concentrations of Cys (A) and GSH (C) excitated at 355 nm. (from bottom to top: 0 μM, 0.5 μM, 1.0 μM, 1.5 μM, 2.0 μM, 2.5 μM, 3.0 μM, 3.5 μM, 4.0 μM, 5.0 μM, 6.0 μM, 7.0 μM, 8.0 μM, 9.0 μM) Inset: Photographs of the N-GQDs/Hg^{2+} containing various concentration of biothiols under UV light. B and D: The linear relationship between $(I-I_0) / I_0$ with the Hg^{2+} concentrations. I_0 and I are the emission fluorescence intensities of N-GQDs at 450 nm in the absence and presence of biothiols, respectively.

(62.19 Wt% C, 3.03 Wt% N and 34.78 Wt% O) were in good agreement with the XPS test.

The prepared N-GQDs were readily water-dispersible due to the presence of hydroxyl and carboxylic groups on the surface and edges, which was confirmed by FT-IR measurement (Figure. S1). N-GQDs exhibited absorption of carboxyl group and hydroxyl group clearly. The absorption band at 3429 cm^{-1} was assigned to O-H and N-H stretching vibration. The absorption band at 1704 cm^{-1} was belonged to C=O stretching vibration of carboxyl group. The strong absorption band at 1597 cm^{-1} was belonged to C=O stretching vibration of acyl amino group. The peak at 1388 cm^{-1} was assigned to C–N stretching vibrations[21, 37]. All these results again confirmed that nitrogen atoms have been successfully doped into N-GQDs.

In order to further explore the optical properties of N-GQDs, UV-vis absorption and fluorescence spectra were recorded. Figure. 3 showed a typical absorption peak at about 353 nm in UV-vis absorption spectra of N-GQDs, which suggested the formation of a graphitic structure in N-GQDs[29]. The maximum excitation peak of N-GQDs was almost the same as the UV-vis absorption peak with the maximum emission at 450 nm. The inset image in Figure. 3 showed the photographs of the N-GQDs under daylight and excitation at 365 nm by a UV lamp. The N-GQDs solution was pale-yellow, transparent under daylight, while emitted strong blue fluorescence under 365 nm. The strong fluorescence of N-GQDs may result from the emissive traps of nitrogen-doped surface[32]. The effect of mass radio of Gly to CA on the fluorescence emission of the N-GQDs was investigated. By using quinine sulfate as a

Figure. 7 Relative fluorescence intensity at maximum excitation wavelength 355 nm of N-GQDs solution in the presence of 10.0 μM of various amino acids. Inset: Photographs of the N-GQDs containing 100 μM of various amino acids under UV light.

reference, the QY of different doping extent N-GQDs were shown in Table. 1. When the mass radio of Gly to CA was 8:2, the fluorescence QY of the obtained N-GQDs was determined to be 28.10%, which was about 7 times higher than that of GQDs. This implied that doping nitrogen to GQDs significantly enhanced the fluorescence QY of GQDs[38].

3.2 The effect of pH on the fluorescence of N-GQDs

The fluorescence intensity of N-GQDs was also dependent on the solution pH. To obtain the optimal analytical conditions for the proposed method, we explored the effect of pH, in the range of 4.0–11.0 on the fluorescence intensities of the N-GQDs in the absence and presence of Hg^{2+} and the kinetic behavior of the reaction. As shown in Figure. 2S, in the absence of Hg^{2+},an obvious enhance in the fluorescence intensity of N-GQDs was observed with a pH increase in the range of 4.0 to 7.0 and the fluorescence intensity of N-GQDs kept smooth in 7.0 to 10.0. The fluorescence intensity of N-GQDs decreased when the pH was above 10.0. The pH dependent character of N-GQDs implied that the protonation state of N-GQDs played an important role in the fluorescence intensity[39]. The optimal fluorescence sensing condition based on N-GQDs was in the pH range of 7.0 to 10.0. However, the quenched fluorescence intensity of the N-GQDs was pH-dependent in the presence of Hg^{2+}, the quenching efficiencies increased strictly with pH from 4.0 to 7.5, then reached maximum at pH 7.5, and then decreased smoothly from pH from 7.5 to 11.0. Thus the experimental condition that followed was set at pH 7.5.

3.3 Selective and sensitive detection of Hg^{2+} ions

The high QY renders N-GQDs a possible type of promising fluorescence probe. So we explored the feasibility of using the N-GQDs for Hg^{2+} detection. The N-GQDs in PBS buffer (10 mM, pH 7.5) displayed strong blue fluorescence, which could be quenched by Hg^{2+}. The fluorescence intensity of N-GQDs gradually decreased with the increasing concentrations of Hg^{2+} and the fluorescence was

Table. 3 Determination results of biothiols in real serum samples

Samples	Reference substance	Determined biothiols (μM)	Added (μM)	Found (μM)	RSD (%,n=3)	Recovery (%)
1	Cys	428.9	300.0	753.0	7.5	103.0
			400.0	824.7	0.9	99.4
			600.0	926.3	2.0	99.2
2	Cys	448.8	300.0	741.2	1.5	97.5
			400.0	850.5	3.2	100.4
			600.0	959.0	1.3	102.0
3	Cys	407.3	300.0	718.9	1.8	103.8
			400.0	828.5	2.6	105.3
			600.0	931.1	7.5	107.4

quenched about 89% by Hg^{2+} at 10 μM (Figure. 4A). The fluorescence intensity change showed a good linear relationship with Hg^{2+} concentration range from 0 μM to 5.0 μM with a liner equation of $(I_0\text{-}I)/I_0$=0.00447+0.132[Hg^{2+}] (R^2=0.9987) (Figure. 4B). The detection limit was calculated to be 0.032 μM with a signal-to-noise ratio (*S*/*N*) of 3, which is relatively lower than those previously reported[40-42]. These results showed that our method based on N-GQDs might be useful in environmental applications for Hg^{2+} detection.

To investigate the selectivity of this sensing system, we tested the fluorescence intensity change of N-GQDs in the presence of representative environmentally relevant metal ions (Ag^{+}, Ba^{2+}, Ca^{2+}, Cd^{2+}, Co^{2+}, Cu^{2+}, Fe^{3+}, Pb^{2+}, Ni^{2+}, Mg^{2+}, Zn^{2+}, Al^{3+}) and Hg^{2+} under the same conditions. 10.0 μM of various ions was added into the N-GQDs solution and the fluorescence response was then recorded. As shown in Figure.7, significant fluorescence quenching effect was observed with the addition of Hg^{2+}, while the other metal ions showed only a slight quenching effect and the influence was almost negligible. The high selectivity of N-GQDs for Hg^{2+} was ascribed to the fact that Hg^{2+} ions have a strong affinity towards the carboxyl groups on the surface of N-GQDs than other ions[20, 22, 42]. The high selectivity of our sensing system for Hg^{2+} indicated the possibility of its application in real samples.

3.4 Assay for real water samples

To demonstrate the practical value of our sensing system, it was used for detecting Hg^{2+} in three real samples. The water samples after pretreatment was spiked with Hg^{2+} at different concentration levels and analyzed with the proposed method. The recovery of Hg^{2+} and the relative standard deviation values were obtained and listed in Table. 2. The result concentrations of Hg^{2+} were in good agreement with the amount of Hg^{2+} spiked. The average quantitative recoveries were 83.0-100.8% with the RSD lower than 7.70%, showing the good accuracy and precision of the established sensing system. Despite the possible inference from the numerous organics and minerals existing in water of the Ming Lake, these results indicated that the proposed method had excellent applicability for Hg^{2+} detection in real samples.

3.5 Selective and sensitive detection of biothiols

On the other hand, the s-donor atoms originated for biothiols such as Cys and GSH exhibits high affinity to Hg^{2+} [20, 43-45]. Hence, upon addition of biothiols in the above N-GQDs/Hg^{2+} system, Hg^{2+} was released from the surface of N-GQDs and the fluorescence of the N-GQDs was recovered. Herein a highly selective fluorescence turn-on method for the detection of biothiols based on N-GQDs/Hg^{2+} was introduced. With the biothiols concentration increasing, a gradual fluorescence increase at 450 nm was observed (Figure. 6A and C). The sensor system displayed the similar response to Cys and GSH.The relationship between the fluorescence intensity and the concentration of Cys (Figure. 6B) showed a liner correlation from 0 μM to 5.0 μM ($(I\text{-}I_0)/I_0$= -0.129+0.528 [Cys], R^2=0.998) with a detection limit of 0.036 μM estimated at S/N=3.. The relationship between the fluorescence intensity and the concentration of GSH (Figure. 6D) showed a liner correlation from 0 μM to 4.5 μM ($(I_0\text{-}I)/I_0$=-0.313+0.566[GSH], R^2=0.992) with a detection limit of 0.034 μM estimated at S/N=3, which are both lower than those previously reported[24, 43, 46].

To investigate the selectivity of N-GQDs/Hg^{2+} system for biothiols, the fluorescence response to various relevant interference amino acids (glycine(Gly), cysteine(Cys), arginine（Arg）, alanine(Ala), serine-(Ser), tryptophan(Try), isoleucine(Ile), proline(Pro), leucine(Leu), glutamic acid(Glu), phenylalanine(Phe), valine(Val), histidine(His)) were tested at the amino acid concentration of 100μM. As shown in Figure. 7, no significant fluorescence recovery appeared with the addition of other common amino acids, except for Cys and GSH, which implied its potential as a selective analytical method for biothiols.

3.6 Assay for real serum samples

In order to evaluate the feasibility of the proposed method in real samples detection, the detection of biothiols in human serums was performed. Generally, the treated serum samples were first diluted 200-fold to fall into the linear range of our method and to enable a quantitative recovery of the spiked biothiols. The total biothiol content in human serum was determined by the standard addition method using Cys as the standard. The obtained biothiols levels were within the reported normal range. In addition, known amounts of Cys were added to the diluted serum samples and the recovery results were ranged from 97.5% to 107.4% with satisfactory RSD

lower than 7.5, indicating a convenient and promising analytical performance for biothiols in serum samples.

4 Conclusion

In summary, high fluorescence N-GQDs were obtained via one-pot pyrolysis using CA and Gly as carbon and nitrogen source respectively with QY of 28.10%. Taking advantage of the excellent fluorescence properties of N-GQDs, a label-free, selective detection method for Hg^{2+} and biothiols was established. The fluorescence "turn-off" sensor for Hg^{2+} was based on the selectively coordination between Hg^{2+} and the functional groups on the surface and edge of N-GQDs. Subsequently, this sensor system was also utilized to detect biothiols (Cys or GSH) based on the high affinity of the sulfur atoms of biothiols to Hg^{2+}. The fluorescence "turn-on" detection was achieved with the addition of biothiols. Both assay (Hg^{2+} and biothiols) exhibited high selectivity, and sensitivity with the detection limits for Hg^{2+}, Cys and GSH to be 0.032 μM, 0.036 μM and 0.034 μM, respectively. We envision that this simple, low-cost synthesized N-GQDs could be further applied in biological and environmental sensing.

Acknowledgements

This work was supported by the National Science Foundation of China (Grant Nos. 51403237), the National Science Foundation of Jiangsu (Grant Nos. BK20140658). College Students Innovation Project for the R&D of Novel Drugs (no.J1030830) and the National College Students' Innovation Entrepreneurial Training Program. B.F.Y. also thanks the Postdoctoral Science Foundation of China and Jiangsu province (Grant Nos. 2014M561544 and 1401036B).

References

1. H. H. Harris, I. J. Pickering and G. N. George, *Science*, 2003, **301**, 1203-1203.
2. F. M. M. Morel, A. M. L. Kraepiel and M. Amyot, *Annual Review Of Ecology And Systematics*, 1998, **29**, 543-566.
3. C. L. He, G. L. Cheng, C. B. Zheng, L. Wu, Y. I. Lee and X. D. Hou, *Anal Methods-Uk*, 2015, **7**, 3015-3021.
4. R. S. Picoloto, H. Wiltsche, G. Knapp, J. S. Barin and E. M. M. Flores, *Anal Methods-Uk*, 2012, **4**, 630-636.
5. M. Leermakers, W. Baeyens, P. Quevauviller and M. Horvat, *Trac - trends in analytical chemistry*, 2005, **24**, 383-393.
6. H. L. Li, J. Y. Liu, Y. X. Fang, Y. A. Qin, S. L. Xu, Y. Q. Liu and E. K. Wang, *Biosensors & Bioelectronics*, 2013, **41**, 563-568.
7. Z. Y. Yao, H. Bai, C. Li and G. Q. Shi, *Chemical Communications*, 2011, **47**, 7431-7433.
8. J. Claus, G. I. Giles, N. M. Giles and S. Helmut, *Angewandte Chemie*, 2003, **35**, 4742–4758.
9. S. Shahrokhian, *Analytical Chemistry*, 2001, **73**, 5972-5978.
10. Q. Y. Xiao, H. L. Gao, C. Lu and Q. P. Yuan, *Trac-Trend Anal Chem*, 2012, **40**, 64-76.
11. J. C. Ndamanisha, J. Bai, B. Qj and L. Guo, *Analytical Biochemistry*, 2009, **386**, 79-84.
12. Z. G. Chen, Z. Wang, J. H. Chen, S. B. Wang and X. P. Huang, *Analyst*, 2012, **137**, 3132-3137.
13. X. Chen, Y. Zhou, X. J. Peng and J. Yoon, *Chemical Society Reviews*, 2010, **39**, 2120-2135.
14. S. Ohmori, T. Kawase, Y. Chisaka, K. Nakata and Y. Yamasaki, *Journal of Chromatography B Biomedical Sciences & Applications*, 2001, **762**, 25–32.
15. H. Genin Gary, X. X. Han, H. Mohammad Kamal and O. Yukihiro, *Analytical Chemistry*, 2009, **81**, 5881-5888.
16. N. Burford, M. D. Eelman, D. E. Mahony and M. Morash, *Chemical Communications*, 2003, **1**, 146-147.
17. D. Tan, Y. He, X. Xing, Y. Zhao, H. Tang and D. Pang, *Talanta*, 2013, **113**, 26-30.
18. J. Zhou, Q. Lu, Y. Tong, W. Wei and S. Q. Liu, *Talanta*, 2012, **99**, 625-630.
19. Y. X. Lu, H. Kong, F. Wen, S. C. Zhang and X. R. Zhang, *Chemical Communications*, 2013, **49**, 81-83.
20. Z. Z. Wu, W. Y. Li, J. Chen and C. Yu, *Talanta*, 2014, **119**, 538-543.
21. B. Shi, L. Zhang, C. Lan, J. Zhao, Y. Su and S. Zhao, *Talanta*, 2015, **142**, 131-139.
22. J. Ju and W. Chen, *Biosensors & Bioelectronics*, 2014, **58**, 219-225.
23. L. A. Ponomarenko, *Science*, 2008, **320**, 356-358.
24. J. Hou, F. S. Zhang, X. Yan, L. Wang, J. Yan, H. Ding and L. Ding, *Analytica chimica acta*, 2015, **859**, 72-78.
25. G. Vinay, C. Neeraj, S. Ritu, S. Gauri Datt, B. Ramil and C. Suresh, *Journal of the American Chemical Society*, 2011, **133**, 9960-9963.
26. J. H. Shen, Y. H. Zhu, C. Chen, X. L. Yang and C. Z. Li, *Chemical Communications*, 2011, **47**, 2580-2582.
27. Y. Li, Y. Hu, Y. Zhao, G. Shi, L. Deng, Y. Hou and L. Qu, *Advanced Materials*, 2011, **23**, 776-780.
28. J. Peng, W. Gao, B. K. Gupta, Z. Liu, R. Romero-Aburto, L. Ge, L. Song, L. B. Alemany, X. Zhan and G. Gao, *Nano Letters*, 2012, **12**, 844-849.
29. Y. Dong, J. Shao, C. Chen, H. Li, R. Wang, Y. Chi, X. Lin and G. Chen, *Carbon*, 2012, **50**, 4738-4743.
30. Y. Li, Y. Zhao, H. H. Cheng, Y. Hu, G. Q. Shi, L. M. Dai and L. T. Qu, *Journal Of the American Chemical Society*, 2012, **134**, 15-18.
31. Q. Q. Li, S. Zhang, L. M. Dai and L. S. Li, *Journal Of the American Chemical Society*, 2012, **134**, 18932-18935.
32. F. Cai, X. D. Liu, S. Liu, H. Liu and Y. M. Huang, *Rsc Advances*, 2014, **4**, 52016-52022.
33. W. Shi, X. Li, H. Ma, Y. Song and W. Chen, *Journal of Materials Chemistry*, 2012, **22**, 12568-12573.
34. L. Li, L. Li, C. Wang, K. Liu, R. Zhu, H. Qiang and Y. Lin, *Microchimica Acta*, 2014, **182**, 763-770.
35. W. Ding, Z. D. Wei, S. G. Chen, X. Q. Qi, T. Yang, J. S. Hu, D. Wang, L. J. Wan, S. F. Alvi and L. Li, *Angew Chem Int Edit*, 2013, **52**, 11755-11759.
36. C. H. Lu, H. H. Yang, C. L. Zhu, X. Chen and G. N. Chen, *Angewandte Chemie International Edition*, 2009, **48**, 4785-4787.
37. G. Fischer, X. Cao, N. Cox and M. Francis, *Chemical Physics*, 2005, **313**, 39–49.
38. H. Sun, N. Gao, L. Wu, J. Ren, W. Wei and X. Qu, *Chemistry-A European Journal*, 2013, **19**, 13362-13368.
39. X. F. Jia, J. Li and E. K. Wang, *Nanoscale*, 2012, **4**, 5572-5575.
40. Y. Y. Xu, L. Deng, H. Wang, X. Y. Ouyang, J. Zheng, J. S. Li and R. H. Yang, *Chemical Communications*, 2011, **47**, 6039-6041.
41. X. J. Xue, F. Wang and X. G. Liu, *Journal Of the American Chemical Society*, 2008, **130**, 3244-+.
42. F. Chai, C. G. Wang, T. T. Wang, Z. F. Ma and Z. M. Su, *Nanotechnology*, 2010, **21**.

43. B. Y. Han, J. P. Yuan and E. K. Wang, *Analytical Chemistry*, 2009, **81**, 5569-5573.
44. K. S. Park, M. I. Kim, M. A. Woo and H. G. Park, *Biosensors & Bioelectronics*, 2013, **45**, 65-69.
45. X. J. Xing, Y. Zhou, X. G. Liu, D. W. Pang and H. W. Tang, *Small*, 2014, **10**, 3412-3420.
46. M. Zhang and B. C. Ye, *Analytical Chemistry*, 2011, **83**, 1504-1509.

The Table of Contents Entry

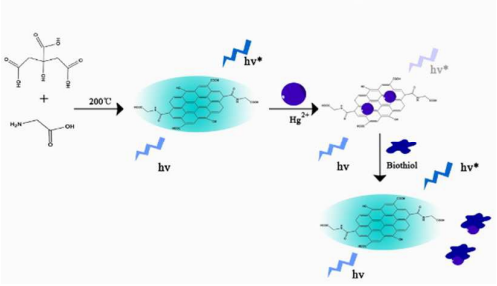

A green synthesis of nitrogen-doped GQDs for the detection of mercury(II) ions and biothiols.